Inorganic Chemistry

Article

pubs.acs.org/IC

Spectroscopic Characterization of Active-Site Variants of the PduO-type ATP:Corrinoid Adenosyltransferase from *Lactobacillus reuteri*: Insights into the Mechanism of Four-Coordinate Co(II)corrinoid Formation

Kiyoung Park,[†] Paola E. Mera,[‡] Jorge C. Escalante-Semerena,[‡] and Thomas C. Brunold*[,†]

[†]University of Wisconsin-Madison, Department of Chemistry, Madison, Wisconsin 53706, United States

[‡]University of Wisconsin-Madison, Department of Bacteriology, Madison, Wisconsin 53706, United States

Supporting Information

ABSTRACT: The PduO-type adenosine 5′-triphosphate (ATP):corrinoid adenosyltransferase from *Lactobacillus reuteri* (*Lr*PduO) catalyzes the transfer of the adenosyl-group of ATP to Co^{1+}cobalamin (Cbl) and Co^{1+}cobinamide (Cbi) substrates to synthesize adenosylcobalamin (AdoCbl) and adenosylcobinamide ($AdoCbi^+$), respectively. Previous studies revealed that to overcome the thermodynamically challenging $Co^{2+} \rightarrow Co^{1+}$ reduction, the enzyme drastically weakens the axial ligand−Co^{2+} bond so as to generate effectively four-coordinate (4c) Co^{2+}corrinoid species. To explore how *Lr*PduO generates these unusual 4c species, we have used magnetic circular dichroism (MCD) and electron paramagnetic resonance (EPR) spectroscopic techniques. The effects of active-site amino acid substitutions on the relative yield of formation of 4c Co^{2+}corrinoid species were examined by performing eight single-amino acid substitutions at seven residues that are involved in ATP-binding, an intersubunit salt bridge, and the hydrophobic region surrounding the bound corrin ring. A quantitative analysis of our MCD and EPR spectra indicates that the entire hydrophobic pocket below the corrin ring, and not just residue F112, is critical for the removal of the axial ligand from the cobalt center of the Co^{2+}corrinoids. Our data also show that a higher level of coordination among several *Lr*PduO amino acid residues is required to exclude the dimethylbenzimidazole moiety of Co(II)Cbl from the active site than to remove the water molecule from $Co(II)Cbi^+$. Thus, the hydrophilic interactions around and above the corrin ring are more critical to form 4c Co(II)Cbl than 4c $Co(II)Cbi^+$. Finally, when ATP analogues were used as cosubstrate, only "unactivated" five-coordinate (5c) Co(II)Cbl was observed, disclosing an unexpectedly large role of the ATP-induced active-site conformational changes with respect to the formation of 4c Co(II)Cbl. Collectively, our results indicate that the level of control exerted by *Lr*PduO over the timing for the formation of the 4c Co^{2+}corrinoid intermediates is even more exquisite than previously anticipated.

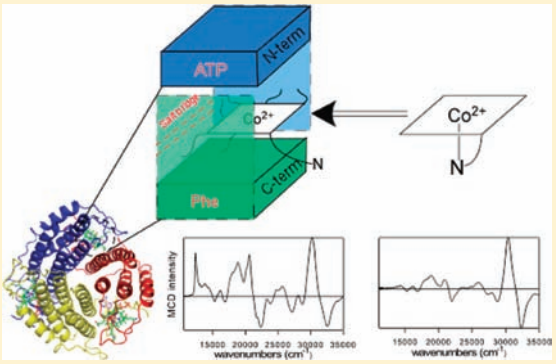

1. INTRODUCTION

The adenosylated derivative of vitamin B_{12}, adenosylcobalamin (AdoCbl), serves as the cofactor in a number of different enzymatic systems.[1] AdoCbl-dependent isomerases, such as methylmalonyl-CoA mutase, glutamate mutase, diol dehydratase, and ethanolamine ammonia lyase, initiate the structural rearrangement of their respective substrates via homolytic cleavage of the Co−C bond of AdoCbl to generate an Ado• radical. Co−C(Ado) bond homolysis also represents the first step in the mechanism of ribonucleotide reduction employed by the AdoCbl-dependent ribonucleotide triphosphate reductase.[2−8] The AdoCbl cofactor used by these enzymes is either synthesized de novo or derived from assimilated exogenous cobalamin species, such as vitamin B_{12} or aquacobalamin (H_2OCbl^+).[9−11] Remarkably, prokaryotes employ more than 25 enzymes to catalyze the stepwise conversion of 5-aminolevulinic acid to AdoCbl via cobalamin precursors such as cobyric acid or cobinamide, the latter of which possesses the complete corrin ring (a tetrapyrrole macrocycle that coordinates the cobalt ion equatorially) but lacks the 5,6-dimethylbenzimidazole (DMB) base on the "lower" face of the corrin ring.[9,11] In contrast, eukaryotes lack the biosynthetic machinery needed to synthesize AdoCbl de novo; instead, they convert assimilated cobalamin species to AdoCbl using ATP:corrinoid adenosyltransferase (ACA) enzymes that transfer the adenosyl group from ATP to the cobalamin substrate.[10,11] Malfunction of the human adenosyltransferase (hATR) can cause methylmalonic aciduria, a fatal disease in infants.[12]

Regardless of whether AdoCbl is synthesized de novo or derived from an external source, an ACA enzyme is required to catalyze the Co−C bond formation step.[9,11,13] Three structurally unrelated and evolutionary distinct classes of

Received: September 26, 2011
Published: April 5, 2012

   dx.doi.org/10.1021/ic202096x | *Inorg. Chem.* 2012, 51, 4482−4494

ACAs can be distinguished, namely, the PduO, CobA, and EutT type enzymes (note that hATR is a member of the PduO class).[4,5,11,13] *Salmonella enterica* (*Se*) contains a member of each of these three classes of ACAs. The *Se*CobA enzyme is employed during the de novo synthesis of AdoCbl and is able to adenosylate cobalamins as well as their incompletely assembled precursors.[9,11] Alternatively, *Se*PduO and *Se*EutT, which are encoded within the *pdu* and *eut* operons, were originally believed to be produced specifically for the assimilation of cobalamins to allow for growth on propanediol and ethanolamine, respectively.[4,5] However, recent studies have revealed that the PduO-type enzyme from *Lactobacillus reuteri* (*Lr*PduO) can in fact also adenosylate cobinamide substrates.[14,15] This finding is particularly intriguing from the point of view that that PduO-type ACAs are utilized by a broad range of organisms, ranging from yeast to humans.[16]

Previous studies of ACAs have revealed that the Co−C(Ado) bond formation step involves a nucleophilic attack on the 5′-carbon of ATP by a transient Co^{1+}corrinoid species that is generated via two separate one-electron reductions of a Co^{3+}corrinoid precursor.[17,18] While the $Co^{3+/2+}$corrinoid reduction potentials are sufficiently positive to ensure that in the reducing environment of the cytoplasm the $Co^{3+} \rightarrow Co^{2+}$corrinoid reduction occurs spontaneously,[19] the $Co^{2+/1+}$corrinoid potentials (e.g., $E°(Co^{2+/1+}Cbl) = -610$ mV vs NHE) are lower than the reduction potentials of readily available in vivo reducing agents (e.g., for the semiquinone/reduced flavin couple of FldA, $E° = -440$ mV vs NHE).[20−22] Nevertheless, this thermodynamically challenging $Co^{2+} \rightarrow Co^{1+}$corrinoid reduction can be accomplished by ACAs.[23−25] In fact, some of us have recently shown that even free dihydroflavins (dihydroriboflavin, $FMNH_2$, and $FADH_2$) can drive the adenosylation of Co(II)Cbl by the human and bacterial PduO-type enzymes, indicating that ACAs are capable of drastically raising the $Co^{2+/1+}$corrinoid potentials.[26] Several different ACA systems have previously been studied using magnetic circular dichroism (MCD) and electron paramagnetic resonance (EPR) spectroscopies, and unique spectral features characterizing ACA-bound Co^{2+}corrinoids in the presence of cosubstrate ATP have been reported.[15,27,28] The appearance of these spectral features was attributed to a significant weakening of the bonding interaction between the axial ligand and the cobalt center, so as to generate effectively four-coordinate (4c) Co^{2+}corrinoid species that possess considerably more positive $Co^{2+/1+}$ reduction potentials than their five-coordinate (5c) counterparts.[27,29,30]

Compelling experimental evidence in support of this proposal was obtained in a recent X-ray crystallographic study of substrate-bound *Lr*PduO.[31] This study revealed that Co^{2+}corrinoids bind near the interface of two subunits of the *Lr*PduO trimer. The "upper" face of the corrinoid is oriented toward a molecule of cosubstrate ATP, which binds to the N-terminal region of one subunit, while the "lower" face is surrounded by hydrophobic residues in the C-terminal region of the adjacent subunit (Figure 1). Most importantly, this structure also shows that a phenylalanine residue, F112, is present below the cobalt center in a region that would otherwise be occupied by an axial ligand to complete the coordination sphere of 5c Co^{2+}corrinoids. In hATR, which is also a PduO-type enzyme that converts its Co^{2+}corrinoid substrate to a 4c species, an analogous phenylalanine residue can be identified (F170).[31,32]

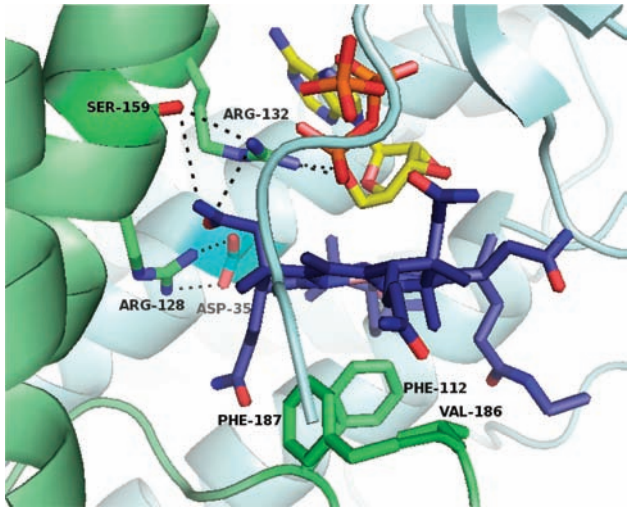

Figure 1. Active-site region of wild type (WT) *Lr*PduO complexed with Co(II)Cbl (blue, center) and cosubstrate ATP (yellow and red, top).[31] Key amino-acid residues are highlighted.

Recently, the insights provided by this crystal structure of *Lr*PduO have been used to prepare a series of variants with substitutions of select active-site residues, and the effect of these substitutions on enzymatic activity, in particular, the rates of Co^{2+}corrinoid reduction and Co^{1+}corrinoid adenosylation, has been determined.[33,34] However, because of the close similarities between the electronic absorption (Abs) spectra of 4c and 5c Co^{2+}corrinoids, it was not possible to correlate enzymatic activity with the relative populations of 4c and 5c Co^{2+}corrinoids that are present in a given sample. Therefore, in this study we have used MCD and EPR spectroscopies to explore how amino acid substitutions influence the ability of *Lr*PduO to generate 4c Co^{2+}corrinoids. Eight point substitutions of seven different residues within the enzyme active site were performed to disturb the ATP-binding region (R132K and S159A), an intersubunit salt bridge (D35N and R128K), and hydrophobic interactions below the corrin ring of the bound corrinoid substrate (F112A, F112H, V186A, and F187A). Studies were conducted with both Co(II)Cbl and the alternative substrate $Co(II)Cbi^+$ to explore how the nature of the axial ligand affects the relative yield of formation of 4c Co^{2+}corrinoid species in the *Lr*PduO active site. Finally, four ATP-analogues (2′-deoxyATP, GTP, CTP, and UTP) were used as cosubstrate to examine if ATP-binding induces conformational changes to the protein that facilitate the formation of 4c Co(II)Cbl.

2. MATERIALS AND METHODS

2.1. Cofactors and Chemicals. The chloride salt of aquacobalamin ($[H_2OCbl]Cl$, >99% pure), dicyanocobinamide ($(CN)_2Cbi$, >93% pure), and sodium borohydride ($NaBH_4$) were purchased from Sigma and used as obtained. Diaquacobinamide ($(H_2O)_2Cbi^{2+}$) was prepared by adding the reductant $NaBH_4$ to an aqueous solution of $(CN)_2Cbi$, loading the reaction mixture on a C18 SepPack column, washing with doubly distilled H_2O, and eluting the product with methanol, as described in a previous report.[27] Co(II)Cbl and $Co(II)Cbi^+$ were prepared by adding $NaBH_4$ to degassed 60% (v/v) glycerol/water solutions of H_2OCbl^+ and $(H_2O)_2Cbi^{2+}$, respectively, and the progress of the reduction was monitored spectrophotometrically.

dx.doi.org/10.1021/ic202096x | *Inorg. Chem.* 2012, 51, 4482−4494

2.2. Protein Preparation and Purification. The protocol used for preparing and purifying variants of *Lr*PduO has been published previously.[35] In short, the variants were generated with the QuickChange XL site-directed mutagenesis kit (Stratagene), where the pTEV3 plasmid carrying the wild-type *Lr* pduO$^+$ allele was used as a template for polymerase chain reaction (PCR)-based site directed mutagenesis. The introduction of the mutations was verified by sequencing the plasmids at the DNA sequence facility of the University of Wisconsin-Madison. The pTEV plasmids encoding the *Lr*PduO variants with a rTEV protease-cleavable N-terminal $(His)_6$ tag were overproduced in *Escherichia coli*, and proteins were isolated using Ni^{2+} affinity chromatography as described elsewhere.[35] All purified proteins were estimated to be >99% homogeneous.

2.3. Sample Preparation. Solutions of *Lr*PduO [in 50 mM Tris-HCl buffer (pH 8) containing 0.5 M NaCl] containing a 1.5−20-fold molar excess of nucleotides (the magnesium salts of ATP or ATP analogues) were degassed at 4 °C before they were combined with the degassed free Co^{2+}corrinoid solutions in a 0.9:1.0 Co^{2+}corrinoid:*Lr*PduO molar ratio in a sealed anaerobic vial. The actual protein concentrations were varied due to differences in the stability of the *Lr*PduO species investigated (see Table S1 for absolute concentrations used). The reaction mixtures, which contained 60% (v/v) glycerol, were then transferred anaerobically into the appropriate sample cells (previously purged with Ar(g)) and immediately frozen in N_2(l).

2.4. Spectroscopy. Magnetic circular dichroism (MCD) spectra were collected on a Jasco J-715 spectropolarimeter in conjunction with an Oxford Instruments SM-4000 8T magnetocryostat. All MCD spectra presented in this paper were obtained by taking the difference between spectra collected with the magnetic field oriented parallel and antiparallel to the light propagation axis to remove contributions from the natural CD and glass strain. X-band EPR spectra were obtained by using a Bruker ESP 300E spectrometer in conjunction with an Oxford ESR 900 continuous-flow liquid helium cryostat and an Oxford ITC4 temperature controller. The microwave frequency was measured with a Varian EIP model 625A CW frequency counter. All spectra were collected using a modulation amplitude of 10 G, a modulation frequency of 100 kHz, and a time constant of 164 ms. EPR spectral simulations were performed with the WEPR program developed by Dr. Neese.[36]

3. RESULTS AND ANALYSIS

3.1. Active-Site Variants. In this study, the effect of active-site amino acid substitutions on the geometric and electronic structures of *Lr*PduO-bound Co^{2+}corrinoids has been examined by MCD and EPR spectroscopic techniques. To enable a direct correlation between spectral changes and perturbations of specific enzyme/substrate interactions, the targeted residues have been classified into three groups: (i) those located above the corrin ring (i.e., near the ATP-binding region), (ii) those situated in the corrin ring plane, and (iii) those positioned below the corrin ring (see Figure 1 and Table 1).

3.2. Substitutions Involving Residues above the Corrin Ring Plane. *3.2.1. R132K.* The guanidinium group of R132 engages in hydrogen-bonding interactions with both cosubstrate ATP and an amide group tethered to the corrin ring (Figure 1). Therefore, R132 likely plays a key role in orienting the C5′ of ATP toward the cobalt center so as to facilitate the Co−C bond formation step.[14,31,33] The positive charge of the guanidinium group may also serve to stabilize the developing negative charge during $Co^{2+} \rightarrow Co^{1+}$Cbl reduction. It is thus not surprising that R132 is conserved among all PduO-type ACAs crystallized to date.[14] In this study, R132 was substituted by a lysine whose side chain is shorter than that of arginine, but retains the ability to participate in H-bond interactions with the phosphate group of ATP.[33]

Table 1. *Lr*PduO Species Investigated

species	perturbation	Co^{2+}corrinoid	$\nu(F1_{4c})$,[a] cm^{-1}	n(4c)/n(tot)[b]
WT *Lr*PduO		Co(II)Cbl	12350	40%
		Co(II)Cbi$^+$	12310	50%
R132K *Lr*PduO	above corrin	Co(II)Cbl	ND[c]	∼0%
	ring	Co(II)Cbi$^+$	12240	19%
S159A *Lr*PduO	above corrin	Co(II)Cbl	12370	13%
	ring	Co(II)Cbi$^+$	12290	39%
R128K *Lr*PduO	in corrin	Co(II)Cbl	12300	5%
	ring plane	Co(II)Cbi$^+$	12220	27%
D35N *Lr*PduO	in corrin	Co(II)Cbl	ND	∼0%
	ring plane	Co(II)Cbi$^+$	12240	23%
F112A *Lr*PduO	below corrin	Co(II)Cbl	ND	∼0%
	ring	Co(II)Cbi$^+$	ND	∼0%
F112H *Lr*PduO	below corrin	Co(II)Cbl	ND	∼0%
	ring	Co(II)Cbi$^+$	ND	∼0%
V186A *Lr*PduO	below corrin	Co(II)Cbl	ND	∼0%
	ring	Co(II)Cbi$^+$	12340	14%
F187A *Lr*PduO	below corrin	Co(II)Cbl	ND	∼0%
	ring	Co(II)Cbi$^+$	12280	6%

[a]Peak position of $F1_{4c}$ feature in corresponding MCD spectrum. [b]Relative yield of formation of 4c Co^{2+}corrinoid. [c]Not detectable.

The MCD spectra of the 4c Co(II)Cbl and Co(II)Cbi$^+$ species bound to the WT *Lr*PduO/ATP complex are characterized by two positively signed prominent features at ∼12300 and ∼20500 cm^{-1}, hereafter referred to as $F1_{4c}$ and $F2_{4c}$, respectively (Figure 2). Both of these features are notably absent in the MCD spectrum of Co(II)Cbl in the presence of the R132K *Lr*PduO variant and cosubstrate ATP (Figure 2a). However, because this spectrum and that of free Co(II)Cbl exhibit small but noticeable differences, it can be concluded that the R132K *Lr*PduO/ATP complex still binds Co(II)Cbl, but no longer requires the axial DMB ligand to dissociate from the Co^{2+} ion.

In contrast to Co(II)Cbl, the substrate analogue Co(II)Cbi$^+$ is still converted to a 4c species when it binds to the R132K *Lr*PduO/ATP complex, as evidenced by the appearance of the $F1_{4c}$ and $F2_{4c}$ features in the corresponding MCD spectrum (Figure 2b). Yet, compared to the MCD spectrum of Co(II)Cbi$^+$ + WT *Lr*PduO/ATP, the intensity of the $F1_{4c}$ feature in this spectrum is lower, while the relative intensity in the ∼15500 − 18500 cm^{-1} region is increased. Both of these differences are consistent with the presence of a larger fraction of 5c Co(II)Cbi$^+$ in the sample of the variant. Notably, the $F1_{4c}$ feature in the spectrum of Co(II)Cbi$^+$ + R132K *Lr*PduO/ATP is red-shifted by 67 cm^{-1} from its counterpart in the spectrum of Co(II)Cbi$^+$ + WT *Lr*PduO/ATP (Table 1). Previously, the $F1_{4c}$ feature of 4c Co^{2+}corrinoids was assigned as a ligand-field (LF) transition involving electronic excitation from the doubly occupied, essentially nonbonding Co $3d_{x^2-y^2}$-based molecular orbital (MO) to the singly occupied, "redox-active" Co $3d_{z^2}$-based MO on the basis of time-dependent density functional

dx.doi.org/10.1021/ic202096x | *Inorg. Chem.* 2012, 51, 4482−4494

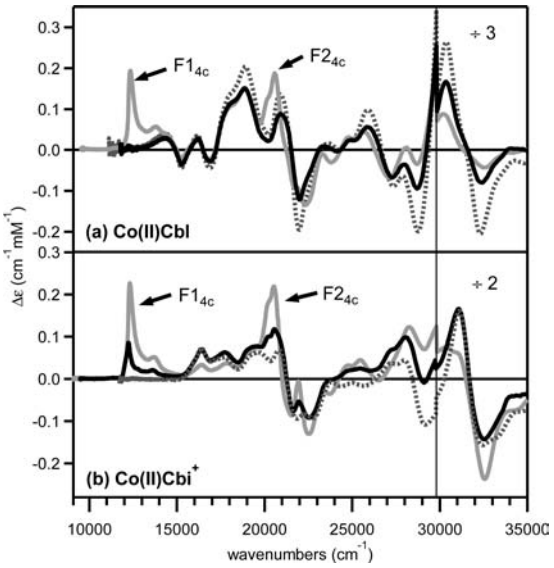

Figure 2. MCD spectra collected at 4.5 K/7 T of (a) free Co(II)Cbl (dotted gray), Co(II)Cbl in the presence of WT *Lr*PduO/ATP (solid gray), and Co(II)Cbl in the presence of R132K *Lr*PduO/ATP (solid black) and of (b) free Co(II)Cbi$^+$ (dotted gray), Co(II)Cbi$^+$ in the presence of WT *Lr*PduO/ATP (solid gray), and Co(II)Cbi$^+$ in the presence of R132K *Lr*PduO/ATP (solid black).

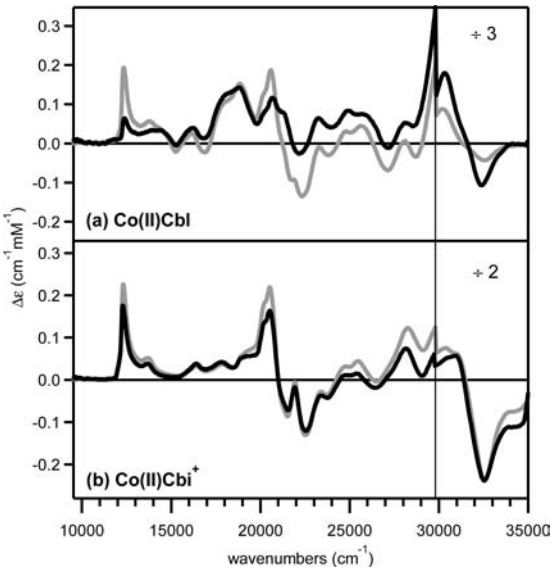

Figure 3. MCD spectra collected at 4.5 K/7 T of (a) Co(II)Cbl in the presence of WT *Lr*PduO/ATP (solid gray) and Co(II)Cbl in the presence of S159A *Lr*PduO/ATP (solid black) and of (b) Co(II)Cbi$^+$ in the presence of WT *Lr*PduO/ATP (solid gray) and Co(II)Cbi$^+$ in the presence of S159A *Lr*PduO/ATP (solid black).

theory (TDDFT) calculations.[27] Given the large separation (~3.0 Å)[31] of the Co^{2+} center from the 5′-carbon of ATP in the WT enzyme, it is unlikely that the R132K substitution causes a further stabilization of the Co $3d_{z^2}$-based MO of *Lr*PduO-bound Co(II)Cbi$^+$. Rather, our data suggest that this substitution leads to a small destabilization of the Co $3d_{x^2-y^2}$-based MO, presumably via corrin-ring deformations.

3.2.2. S159A. Located above the corrin ring adjacent to R132, S159 is another universally conserved active-site residue among the PduO-type ACAs discovered so far.[14] While this residue does not directly interact with enzyme-bound ATP, it is hydrogen-bonded to one of the amide groups of the corrin ring as well as to the guanidinium group of R132 (Figure 1). Hence, the S159A substitution is expected to cause subtle changes in the relative positioning of the two substrates.

The MCD spectra of Co(II)Cbl and Co(II)Cbi$^+$ in the presence of S159A *Lr*PduO and ATP both show the F1$_{4c}$ and F2$_{4c}$ features characteristic of 4c Co^{2+}corrinoids (Figure 3). However, the intensity of the F1$_{4c}$ feature in the MCD spectrum of Co(II)Cbl + S159A *Lr*PduO/ATP is significantly decreased from that obtained for Co(II)Cbl + WT *Lr*PduO/ATP (Figure 3a), signifying a lower yield of conversion from 5c to 4c Co(II)Cbl in the variant. In contrast, the MCD spectra of Co(II)Cbi$^+$ bound to the S159A and WT *Lr*PduO/ATP complexes are nearly identical (Figure 3b); hence, the S159A substitution does not hinder the conversion of this alternative substrate to a 4c species. Yet, the F1$_{4c}$ and F2$_{4c}$ features of the 4c Co(II)Cbi$^+$ species bound the S159A *Lr*PduO/ATP complex are down-shifted by 22 and 25 cm^{-1}, respectively, from those in the WT *Lr*PduO/ATP complex, indicating that the Co(II)Cbi$^+$/enzyme interaction is slightly perturbed by the S159A substitution.

3.3. Substitutions Involving Residues in the Corrin Ring Plane. *3.3.1. R128K.* R128 is another conserved residue among PduO-type ACAs.[14,31,33] In WT *Lr*PduO, the guanidinum group of R128 forms a pair of hydrogen bonds with the carboxylate group of D35, which is located in the adjacent subunit (Figure 1). To test the possibility that this salt bridge assists in the formation of 4c Co^{2+}corrinoids, we replaced the R128 residue by a lysine, which features a shorter side chain than arginine and a single $-NH_3^+$ group that can engage in hydrogen-bond interactions.

The MCD spectrum of Co(II)Cbl in the presence of R128K *Lr*PduO and ATP (Figure 4a) shows a small but distinct F1$_{4c}$ feature at 12300 cm^{-1}, indicating that in this variant only a minor fraction of Co(II)Cbl is converted to a 4c species. Similarly, the MCD spectrum of Co(II)Cbi$^+$ in the presence of

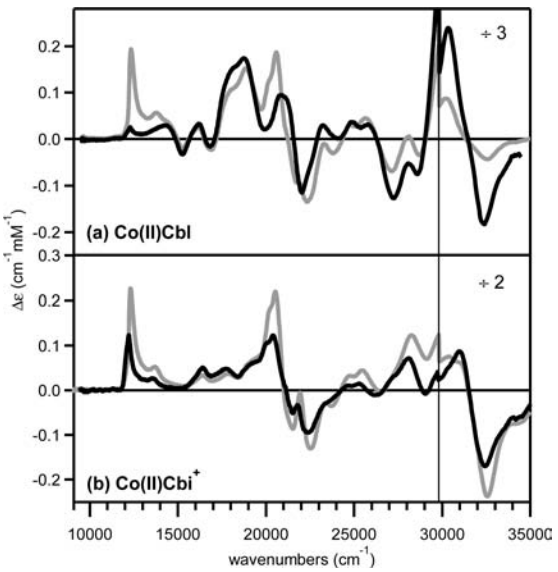

Figure 4. MCD spectra collected at 4.5 K/7 T of (a) Co(II)Cbl in the presence of WT *Lr*PduO/ATP (solid gray) and Co(II)Cbl in the presence of R128K *Lr*PduO/ATP (solid black) and of (b) Co(II)Cbi$^+$ in the presence of WT *Lr*PduO/ATP (solid gray) and Co(II)Cbi$^+$ in the presence of R128K *Lr*PduO/ATP (solid black).

dx.doi.org/10.1021/ic202096x | *Inorg. Chem.* 2012, 51, 4482–4494

the R128K *Lr*PduO variant contains substantial contributions from 5c Co(II)Cbi$^+$ and, therefore, exhibits a weaker $F1_{4c}$ feature than the Co(II)Cbi$^+$ + WT *Lr*PduO/ATP spectrum (Figure 4b). Notably, the $F1_{4c}$ features of the 4c Co(II)Cbl and Co(II)Cbi$^+$ fractions in the R128K *Lr*PduO/ATP complex are red-shifted by 46 and 90 cm^{-1}, respectively, from those of their counterparts in the WT *Lr*PduO/ATP complex. As described above for the R132K substitution, these shifts likely reflect a destabilization of the Co $3d_{x^2-y^2}$-based MO in response to the R128K substitution, suggesting that a (partial) rupture of the salt bridge between R128 and D35 causes a distortion of the corrin ring that renders the Co $3d_{x^2-y^2}$-based MO slightly more antibonding with respect to the Co−N(corrin) bonds (note that the suggested protein conformational changes are too subtle to be detectible by CD spectroscopy).

3.3.2. D35N. A complementary means to perturb this intersubunit salt bridge is to replace the hydrogen-bond acceptor, D35, which is also conserved among PduO-type ACAs.[14,31,33] Therefore, the D35N *Lr*PduO variant was prepared and its interaction with Co^{2+}corrinoids was examined by MCD spectroscopy. The absence of the $F1_{4c}$ feature in the MCD spectrum of Co(II)Cbl + D35N *Lr*PduO/ATP indicates that that the D35N substitution completely abolishes the formation of 4c Co(II)Cbl (Figure 5a). It does not, however, appear to prevent Co(II)Cbl from binding to the enzyme active site, as the MCD spectrum of Co(II)Cbl + D35N *Lr*PduO/ATP is quite different from that of free Co(II)Cbl, especially in the 17000−22000 cm^{-1} and 23000−30000 cm^{-1} regions (Figure 5a). Collectively, these results suggest that the D35N substitution relieves some of the steric constraints imposed on the active site-bound Co(II)Cbl species and thus allows it to retain its axial DMB base.

As expected on the basis of the results obtained for R128K *Lr*PduO, the D35N substitution also lowers the yield of formation of enzyme-bound 4c Co(II)Cbi$^+$, as revealed by the decreased intensity of the $F1_{4c}$ feature in the MCD spectrum of Co(II)Cbi$^+$ + D35N *Lr*PduO/ATP (Figure 5b). Further evidence for a perturbed Co(II)Cbi$^+$/enzyme interaction in this variant is provided by the fact that the $F1_{4c}$ feature of the 4c fraction is red-shifted by 69 cm^{-1} from its position in the Co(II)Cbi$^+$ + WT *Lr*PduO/ATP spectrum.

3.4. Substitutions Involving Residues below the Corrin Ring Plane. *3.4.1. F112A and F112H.* The X-ray crystal structures of the *Lr*PduO/ATP complex in the absence and presence of Co(II)Cbl revealed that the C-terminus that is disordered in the substrate-free enzyme becomes ordered upon Co(II)Cbl-binding and a phenylalanine residue (F112, which is conserved among the PduO-type ACAs) moves to within 3.8 Å of the Co^{2+} ion. On the basis of these observations it was proposed that F112 serves to promote the dissociation of the axial ligand that would otherwise be present to complete the coordination sphere of 5c Co^{2+}corrinoids (Figure 1).[31] To test this proposal, two variants of *Lr*PduO were prepared in which the phenyl group of the F112 residue was either removed (F112A) or substituted with a potentially coordinating heteroaromatic moiety (F112H).

The MCD spectrum of Co(II)Cbl in the presence of F112A *Lr*PduO and ATP lacks the $F1_{4c}$ feature characteristic of 4c Co^{2+}corrinoids and instead closely resembles the MCD spectrum of free Co(II)Cbl (Figure 6a). Because the *Lr*PduO active site does not contain any His residues, this result indicates that Co(II)Cbl retains its DMB ligand in the presence of the F112A *Lr*PduO/ATP complex. However, several lines of evidence suggest that the F112A substitution does not prevent Co(II)Cbl from binding to the *Lr*PduO active site. First, compared to the free Co(II)Cbl MCD spectrum, the features between 13000 and 15500 cm^{-1} are weaker and those in the ∼15500−21000 cm^{-1} region are shifted by up to 50 cm^{-1} in the Co(II)Cbl + F112A *Lr*PduO/ATP spectrum. Second, the relative intensities of the MCD features in the 23000−26500 cm^{-1} region, previously attributed to corrin $\pi \rightarrow \pi^*$ transitions, are considerably altered by the addition of the F112A *Lr*PduO/ATP complex to Co(II)Cbl, and the maximum of the positively

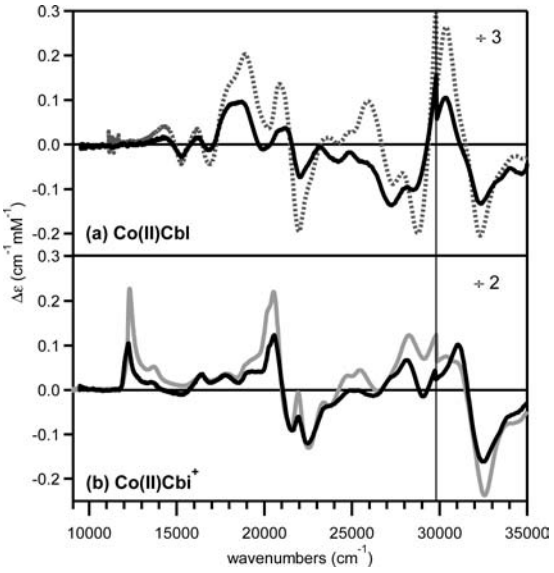

Figure 5. MCD spectra collected at 4.5 K/7 T of (a) free Co(II)Cbl (dotted gray) and Co(II)Cbl in the presence of D35N *Lr*PduO/ATP (solid black) and of (b) Co(II)Cbi$^+$ in the presence of WT *Lr*PduO/ATP (solid gray) and Co(II)Cbi$^+$ in the presence of D35N *Lr*PduO/ATP (solid black).

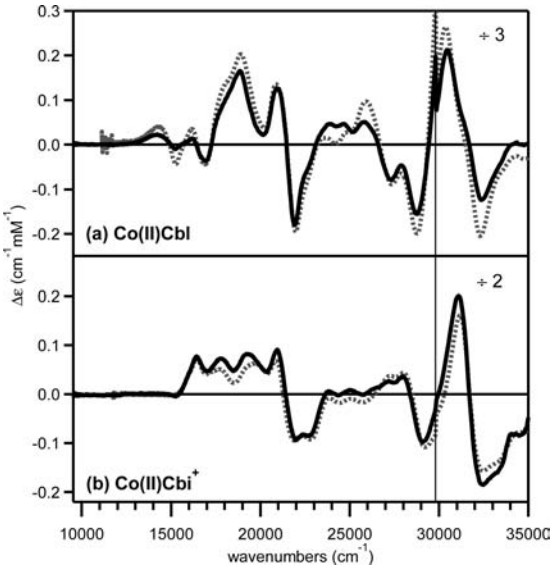

Figure 6. MCD spectra collected at 4.5 K/7 T of (a) free Co(II)Cbl (dotted gray) and Co(II)Cbl in the presence of F112A *Lr*PduO/ATP (solid black) and of (b) free Co(II)Cbi$^+$ (dotted gray) and Co(II)Cbi$^+$ in the presence of F112A *Lr*PduO/ATP (solid black).

dx.doi.org/10.1021/ic202096x | *Inorg. Chem.* 2012, 51, 4482−4494

signed component of the derivative-shaped MCD feature centered at 30500 cm^{-1} is blue-shifted by ~140 cm^{-1} (Figure 6a). Third, the EPR spectrum of Co(II)Cbl + F112A *Lr*PduO/ATP shows fine structure at 2989, 3066, and 3086 G that is absent in the spectrum of free Co(II)Cbl (cf. Figure 7a,b).

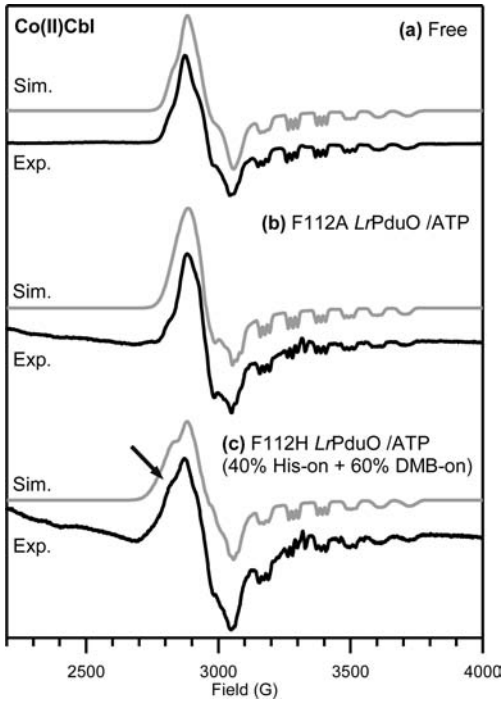

Figure 7. EPR spectra collected at 20 K of (a) free Co(II)Cbl, (b) Co(II)Cbl in the presence of F112A *Lr*PduO/ATP, and (c) Co(II)Cbl in the presence of F112H *Lr*PduO/ATP (the arrow points to the shoulder at 2824 G that is due to the DMB-off/His-on Co(II)Cbl species). The simulated spectrum in (c) was obtained by adding the spectral simulations in Figure 9c and Figure 7a in a 0.4:0.6 intensity ratio.

Additionally, EPR spectral simulations indicate that the former spectrum is more axial, as revealed by the smaller difference between the fitted g_2 and g_3 values (Table 2). This finding

Table 2. EPR *g*-Values and ^{59}Co Hyperfine Values $A(^{59}Co)$ (in MHz) Used for Spectral Simulations in Figures 7 and 9

species	g_1	g_2	g_3	$A_1(^{59}Co)$	$A_2(^{59}Co)$	$A_3(^{59}Co)$
free Co(II)Cbl	2.004	2.230	2.280	305	30	40
free Co(II)Cbi$^+$	2.005	2.350	2.350	410	240	240
Co(II)Cbl + F112A *Lr*PduO/ATP	2.005	2.260	2.265	299	48	55
H112-on Co(II)Cbi$^+$ /Co(II)Cbl	2.003	2.295	2.305	315	90	73

implies that the energetic splitting between the Co $3d_{yz}$- and $3d_{xz}$-based MOs of Co(II)Cbl decreases upon the addition of the F112A *Lr*PduO/ATP complex, consistent with the apparent decrease in intensity of the MCD features between 13000 and 15500 cm^{-1} that have previously been assigned as LF transitions originating from the Co $3d_{xz}$- and $3d_{yz}$-based MOs (since these transitions are oppositely signed in the MCD spectrum, their intensities will decrease as the two donor orbitals shift closer in energy).[29,37] Collectively, these observations indicate that the active site of F112A *Lr*PduO is large enough to accommodate DMB-on Co(II)Cbl even in the presence of cosubstrate ATP and suggest that the corrin ring conformation, and thus the corrin $\pi\rightarrow\pi^*$ transitions, are slightly perturbed in the enzyme-bound Co(II)Cbl species.

A comparison of the MCD spectra of Co(II)Cbi$^+$ in the absence and presence of F112A *Lr*PduO/ATP shows minor differences in the 17000−20000 cm^{-1} region attributed to Co^{2+}-centered LF transitions and a red-shift by ~100 cm^{-1} of the most intense positively signed MCD feature at 31100 cm^{-1} (Figure 6b). Hence, it can be concluded that Co(II)Cbi$^+$, similar to Co(II)Cbl, also retains its axial ligand when it binds to the active site of F112A *Lr*PduO containing ATP.

Judging from the X-ray crystal structure of WT *Lr*PduO with both ATP and Co(II)Cbl present, the imidazole group of the H112 residue in the F112H *Lr*PduO variant should be properly positioned to coordinate axially to enzyme-bound Co(II)Cbl, provided the F112H substitution does not severely perturb the overall protein conformation. However, since both the DMB and imidazole groups are nitrogen-donors with comparable electron donating abilities, substitution of the axial DMB ligand of Co(II)Cbl by a protein-derived histidine residue is difficult to discern spectroscopically. It is thus not surprising that the MCD spectra of Co(II)Cbl in the absence and presence of F112H *Lr*PduO/ATP are very similar, though small differences are observed, especially with regard to the band positions in the 13000−20000 cm^{-1} region and the intensity of the ~20900 cm^{-1} feature associated with the lowest-energy corrin $\pi \rightarrow \pi^*$ transition (Figure 8a). Likewise, the EPR spectrum of Co(II)Cbl is only weakly perturbed by the addition of F112H *Lr*PduO/ATP, the most notable change being the appearance of a shoulder (at 2824 G) on the low-field side of the feature at 2878 G (see arrow in Figure 7c). The relative

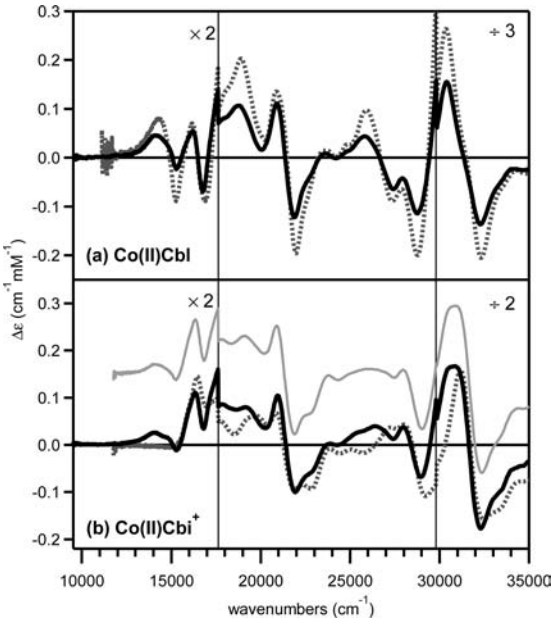

Figure 8. MCD spectra collected at 4.5 K/7 T of (a) free Co(II)Cbl (dotted gray) and Co(II)Cbl in the presence of F112H *Lr*PduO/ATP (solid black) and of (b) free Co(II)Cbi$^+$ (dotted gray) and Co(II)Cbi$^+$ in the presence of F112H *Lr*PduO/ATP (solid black). The simulated spectrum in (b) (solid gray, offset for clarity) was obtained by adding the MCD spectra of Co(II)Cbi$^+$ and Co(II)Cbl + F112H *Lr*PduO/ATP in a 0.6:0.4 ratio.

dx.doi.org/10.1021/ic202096x | *Inorg. Chem.* 2012, 51, 4482−4494

intensity of this shoulder was found to vary depending on the sample concentration used (Figure S1, Supporting Information), indicating that two different species are present in these samples. From a comparison to the EPR data obtained for Co(II)Cbi$^+$ in the presence of F112H *Lr*PduO/ATP (see below), we attribute the feature at 2824 G in the EPR spectrum of Co(II)Cbl + F112H *Lr*PduO/ATP to an enzyme-bound DMB-off/His-on Co(II)Cbl species that represented ∼40% of the total amount of Co(II)Cbl in this particular sample.

Because axial histidine versus H_2O coordination in Co^{2+}corrinoids can be readily distinguished on the basis of MCD and EPR spectra,[29] we also investigated the interaction between Co(II)Cbi$^+$ and the F112H *Lr*PduO variant. The fact that the MCD spectrum of Co(II)Cbi$^+$ + F112H *Lr*PduO/ATP differs substantially from that of free Co(II)Cbi$^+$ (Figure 8b) and instead exhibits a number of features that are also observed in the MCD spectrum of Co(II)Cbl + F112H *Lr*PduO/ATP (Figure 8a) provides compelling evidence for H112 coordination to enzyme-bound Co(II)Cbi$^+$. By fitting the MCD spectrum of Co(II)Cbi$^+$ + F112H *Lr*PduO/ATP using a combination of the spectra of free Co(II)Cbi$^+$ and Co(II)Cbl + F112H *Lr*PduO/ATP, it was found that ∼40% of the Co(II)Cbi$^+$ species in this particular sample were ligated by H112 (Figure 8b).

Consistent with our MCD data, the EPR spectrum of Co(II)Cbi$^+$ + F112H *Lr*PduO/ATP (Figure 9a) exhibits a prominent feature at ∼2802 G that has no counterpart in the spectrum of free Co(II)Cbi$^+$ (Figure 9b) but instead closely mirrors the dominant peak in the free Co(II)Cbl EPR spectrum (Figure 7c). Additionally, well-resolved triplets due to superhyperfine coupling to an axially ligated ^{14}N atom are discernible in the 3100−3800 G region of the Co(II)Cbi$^+$ + F112H *Lr*PduO/ATP spectrum (Figure 9a). To generate a "pure" EPR spectrum of the His-on bound fraction of Co(II)Cbi$^+$ in this sample, a suitably scaled spectrum of free Co(II)Cbi$^+$ (Figure 9b) was subtracted from the trace in Figure 9a; the resulting difference spectrum is shown in Figure 9c. This analysis revealed that ∼40% of the Co(II)Cbi$^+$ species in this sample were converted to the His-bound form, in excellent agreement with the results obtained from the MCD spectral analysis presented above. Interestingly, the "pure" His-on Co(II)Cbi$^+$ + F112H *Lr*PduO/ATP spectrum is characterized by g_2 and g_3 values that are larger, and more similar to one another, than those associated with free Co(II)Cbl (Table 2). Considering that the g_2 and g_3 values increase in response to a weakening of the bonding interaction between the Co^{2+} center and the axial ligand,[27] this finding likely suggests that the motion of the H112 side chain in the F112H *Lr*PduO variant is restricted by the protein backbone, thus causing the Co−N(H112) bond to be longer than the Co−N(DMB) bond of free Co(II)Cbl.

3.4.2. V186A. Located between two phenylalanine residues, F112 and F187, V186 likely serves to enhance the hydrophobic character of the area below the corrin ring (Figure 1). To evaluate the importance of this residue in restricting access of polar molecules to the enzyme active site and the role it plays in the formation of 4c Co^{2+}corrinoids, the V186A *Lr*PduO variant was prepared.

The MCD spectrum of Co(II)Cbl in the presence of V186A *Lr*PduO and ATP (Figure 10a) lacks the $F1_{4c}$ feature associated with 4c Co(II)Cbl, even though the F112 residue is still present in this variant. In fact, this spectrum is more similar to that of free Co(II)Cbl than of Co(II)Cbl + WT *Lr*PduO devoid of ATP, suggesting that Co(II)Cbl may not actually bind to V186A *Lr*PduO. In contrast, the MCD spectrum of Co(II)Cbi$^+$ + V186A *Lr*PduO/ATP clearly shows the $F1_{4c}$ feature of 4c Co(II)Cbi$^+$, albeit up-shifted by 30 cm^{-1} and considerably reduced in intensity from its counterpart in the Co(II)Cbi$^+$ + WT *Lr*PduO/ATP spectrum (Figure 10b and Table 1). Hence,

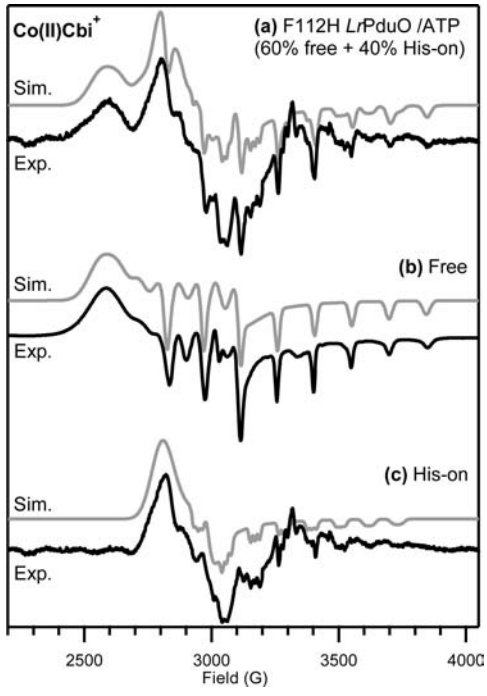

Figure 9. EPR spectra collected at 20 K of (a) Co(II)Cbi$^+$ in the presence of F112H *Lr*PduO/ATP and (b) free Co(II)Cbi$^+$. The spectrum in (c) of the H112-bound fraction of Co(II)Cbi$^+$ in F112H *Lr*PduO/ATP was obtained as described in the text.

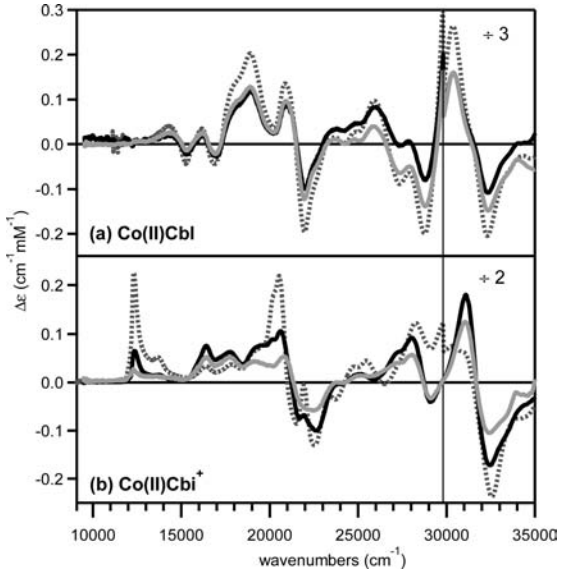

Figure 10. MCD spectra collected at 4.5 K/7 T of (a) free Co(II)Cbl (dotted gray), Co(II)Cbl + V186A *Lr*PduO/ATP (solid black), and Co(II)Cbl + F187A *Lr*PduO/ATP (solid gray) and of (b) Co(II)Cbi$^+$ + WT *Lr*PduO/ATP (dotted gray), Co(II)Cbi$^+$ + V186A *Lr*PduO/ATP (solid black), and Co(II)Cbi$^+$ + F187A *Lr*PduO/ATP (solid gray).

dx.doi.org/10.1021/ic202096x | *Inorg. Chem.* 2012, 51, 4482−4494

the active site of the V186A variant remains sufficiently hydrophobic to promote dissociation of the axially bound water molecule from at least a fraction of the enzyme-bound Co(II)Cbi$^+$ species.

3.4.3. F187A. Similar to V186, the F187 residue is located below the corrin ring in close proximity to F112 (Figure 1) and is another key building block of the hydrophobic wall between the active site and solvent. Consistent with the similar roles played by these two residues, the MCD spectra of Co(II)Cbl and Co(II)Cbi$^+$ in the presence of F187A *Lr*PduO and ATP closely resemble those obtained for the V186A variant (Figure 10). One notable difference, though, is that the F187A substitution causes the $F1_{4c}$ feature of 4c Co(II)Cbi$^+$ to down-shift, rather than to upshift (Table 1). This finding suggests that the V186A and F187A substitutions induce somewhat different changes in the corrin ring conformation of enzyme-bound Co(II)Cbi$^+$.

3.5. Variations in the Cosubstrate. While the R132K substitution permitted us to evaluate the effect of a perturbed interaction between the phosphate group of ATP and the *Lr*PduO active site on the yield of formation of 4c Co^{2+}corrinoids (see above), ATP analogues were used to assess the importance of the remaining hydrogen-bond interactions between ATP and the protein. According to the X-ray crystal structure of *Lr*PduO containing ATP and Co(II)Cbl, the adenosine moiety of ATP engages in hydrogen-bond interactions with two adjacent protein subunits, on one side via the 2′-OH group of the ribose ring with the backbone carbonyl group of R14 and the hydroxyl group of Y31, and on the other side via the amino group attached to C6 of the adenine with the backbone carbonyl group of R132 on the adjacent subunit (Figure 1).[14,31,33] The importance of these hydrogen-bond interactions with the two different protein subunits was evaluated separately by using 2′-deoxyATP (2′-dATP) and guanosine-5′-triphosphate (GTP, which possesses an oxo group at C6), respectively. Additionally, the pyrimidine nucleotides cytidine-5′-triphosphate (CTP) and uridine-5′-triphosphate (UTP) were employed to examine the effect of a change in base size on the Co(II)Cbl/enzyme interaction.

3.5.1. Purine Nucleotides. The MCD spectrum of Co(II)-Cbl in the presence of WT *Lr*PduO and 2′-dATP lacks the $F1_{4c}$ feature of 4c Co(II)Cbl (Figure 11a), even though recent kinetic studies revealed that *Lr*PduO converts Co(I)Cbl$^-$ to AdoCbl using 2′-dATP at similar rates as it does with ATP.[33] This spectrum does, however, exhibit noticeable differences from that of free Co(II)Cbl (Figure 11a), indicating that both 2′-dATP and Co(II)Cbl bind to the enzyme active site. Thus, we conclude that the interaction between the 2′-OH group of ATP and the protein is critical for the formation of 4c Co(II)Cbl, but not for the adenosylation of Co(I)Cbl$^-$.

In contrast, the MCD spectrum of Co(II)Cbl in the presence of WT *Lr*PduO and GTP shows that 4c Co(II)Cbl is formed in this case (Figure 11a), albeit in low yield since the intensity of the $F1_{4c}$ feature is only ~8% of that observed when ATP is used instead (Figure S3). The remaining features in the MCD spectrum of Co(II)Cbl + WT *Lr*PduO/GTP are largely due to the 5c fraction of Co(II)Cbl, which also seems to be bound to the enzyme active site considering that the features in the 23000−29500 cm^{-1} region associated with corrin $\pi \rightarrow \pi^*$ transitions are similarly perturbed in this spectrum and the spectrum obtained with 2′-dATP (Figure 11a).

3.5.2. Pyrimidine Nucleotides. CTP is a pyrimidine nucleotide that possesses an amino group at C4 and an oxo group at C2. Apparently, these structural deviations from ATP are sufficiently large to prevent Co(II)Cbl from binding to the WT *Lr*PduO/CTP complex, since the corresponding MCD spectrum is essentially identical to that of free Co(II)Cbl (Figure 11b). In contrast, clear differences are observed between the MCD spectra of Co(II)Cbl and WT *Lr*PduO in the absence and presence of UTP, which differs from CTP by the presence of an oxo group at C4 (Figure 11b). Interestingly, the MCD spectrum of Co(II)Cbl + WT *Lr*PduO/UTP is most similar to that of Co(II)Cbl + D35N *Lr*PduO/ATP (Figure 5a), suggesting that the ATP base/protein interactions play a similar role as the salt bridge between two subunits with respect to the proper organization of the *Lr*PduO active site.

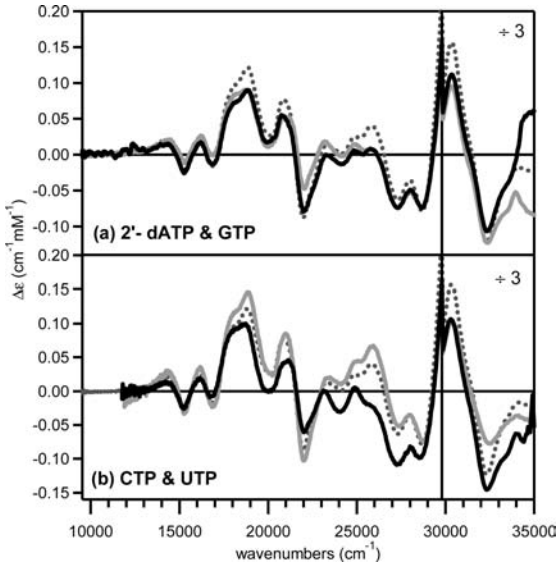

Figure 11. MCD spectra collected at 4.5 K/7 T of (a) Co(II)Cbl + WT *Lr*PduO (dotted gray), Co(II)Cbl + WT *Lr*PduO/2′-deoxyATP (solid gray), and Co(II)Cbl + WT *Lr*PduO/GTP (solid black) and of (b) Co(II)Cbl + WT *Lr*PduO (dotted gray), Co(II)Cbl + WT *Lr*PduO/CTP (solid gray), and Co(II)Cbl + WT *Lr*PduO/UTP (solid black).

4. DISCUSSION

4.1. Effects of Amino-Acid Substitutions on Co^{2+}Corrinoid/Enzyme Interactions. Previous DFT and time-dependent density functional theory (TDDFT) computational studies performed by some of us revealed that the MCD spectra of Co^{2+}corrinoids can be divided into three distinct regions according to the nature of the underlying electronic transitions (Figure 12).[27,29,37] The low-energy region (<17500 cm^{-1}) is dominated by LF transitions involving electronic excitations among the Co 3d-based MOs, while the major features in the high-energy region (>21000 cm^{-1}) are due to corrin-centered $\pi \rightarrow \pi^*$ transitions. The most intense features observed between these two regions arise from electronic excitations between Co 3d-based and corrin π^*-based MOs, corresponding to metal-to-ligand charge transfer (MLCT) transitions (Figure 12). While it is nearly impossible to make specific assignments of all MCD bands because of the vast number of available donor and acceptor MOs for electronic transitions, the $F1_{4c}$ feature of 4c Co^{2+}corrinoids could be assigned conclusively to the Co $3d_{x^2-y^2} \rightarrow 3d_{z^2}$ LF transition on the basis of experimentally calibrated TDDFT calculations.[27]

dx.doi.org/10.1021/ic202096x | *Inorg. Chem.* 2012, 51, 4482−4494

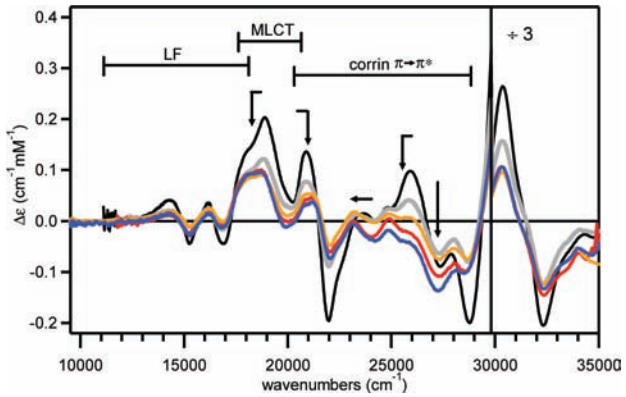

Figure 12. MCD spectra collected at 4.5 K/7 T of free Co(II)Cbl (black) and of Co(II)Cbl in the presence of WT *Lr*PduO (gray), WT *Lr*PduO/UTP (red), WT *Lr*PduO/2′-dATP (orange), and D35N *Lr*PduO/ATP (blue). Arrows indicate the major spectral changes in the MLCT and corrin $\pi \rightarrow \pi^*$ transition regions along this series of spectra.

4.1.1. Distortion of Corrin Ring. In the present study, the MCD spectra of the 5c, DMB-on Co(II)Cbl species in the various samples investigated were found to vary quite substantially. The largest deviations from the free Co(II)Cbl spectrum are displayed by samples containing Co(II)Cbl and either D35N *Lr*PduO/ATP or WT *Lr*PduO plus the alternative nucleotides UTP or 2′-dATP (Figure 12). Qualitatively similar, albeit less pronounced MCD spectral changes were observed previously upon Co(II)Cbl binding to WT *Lr*PduO devoid of ATP.[15] Interestingly, these changes occur mainly in the regions associated with MLCT and corrin $\pi \rightarrow \pi^*$ transitions, while the LF transitions remain largely unperturbed. Thus, these changes cannot be attributed to the formation of any sizable fraction of base-off or 4c Co(II)Cbl, because in that case the LF region would also be perturbed. We therefore conclude that a moderate distortion of the corrin ring occurs upon Co(II)Cbl binding to WT *Lr*PduO and that this distortion becomes more pronounced when Co(II)Cbl binds to the D35N *Lr*PduO/ATP complex or WT *Lr*PduO containing UTP or 2′-dATP. Indirect support for this proposal comes from an analysis of the X-ray crystal structure of Co(II)Cbl + WT *Lr*PduO/ATP,[31] which shows that the D35N substitution and the replacement of ATP by 2′-dATP should similarly, and quite strongly, perturb the hydrogen-bond interactions between the two protein subunits near the Co^{2+}corrinoid binding site. Note that because $Co(II)Cbi^+$ is still converted to a 4c species upon binding to the D35N *Lr*PduO/ATP complex, it is extremely unlikely that the MCD spectrum shown in Figure 12 reflects nonspecific binding of Co(II)Cbl to this variant.

For decades the corrin ring has been recognized for its increased flexibility over the porphyrin macrocycle, which allows it to fold, or unfold, depending on the bulkiness of the axial ligand(s) bound to the central cobalt ion.[30,38−42] The extent of these conformational changes can be expressed in terms of the corrin fold angle ϕ, defined here as the angle between the planes formed by N21−C1−C19−N24 and N22−C9−C10−C11−N23 so as to quantify folding along the "long" axis (C5···C15 vector) of the corrin ring (Figure S4). As expected, the corrin fold angle in free, DMB-on Co(II)Cbl (ϕ = 14.5°)[43] is larger than in the 4c Co(II)Cbl species formed in the WT *Lr*PduO/ATP complex (ϕ = 5.7°).[31] However, the more planar corrin ring conformation in the enzyme-bound species may in fact be due to the steric constraints imposed by active-site residues located above and below the macrocycle, rather than the absence of bulky axial ligands. Indeed, the MCD spectra of the 5c, DMB-on faction of Co(II)Cbl bound to variants of *Lr*PduO (+ATP) in which the steric crowding below the corrin ring is reduced, such as by the F112A, V186A, or F187A substitutions, are more similar to the MCD spectrum of free Co(II)Cbl than of Co(II)Cbl + WT *Lr*PduO devoid of ATP (Figure 12). Moreover, as discussed above, the distortion of the corrin ring is most substantial in the 5c, DMB-on Co(II)Cbl species bound to the D35N *Lr*PduO/ATP complex, where the steric crowding present in WT *Lr*PduO devoid of ATP is preserved and additional geometric constraints are introduced by the presence of cosubstrate ATP. Collectively, these findings suggest that the MCD spectral changes in the regions associated with MLCT and corrin $\pi \rightarrow \pi^*$ transitions between free and *Lr*PduO-bound Co(II)Cbl species actually reflect a flattening, rather than a folding, of the corrin ring. According to this scenario, the corrin ring would be most planar in Co(II)Cbl bound to the D35N *Lr*PduO/ATP complex, which seems reasonable because in this species the DMB ligand as well as all of the bulky residues below the corrin ring plane are present in the active site, likely forcing an upward motion of the Co^{2+} ion and, thus, a decrease in ϕ.

4.1.2. Perturbations to ATP Binding Region. The MCD spectrum of Co(II)Cbl + R132K *Lr*PduO/ATP (Figure 2) is almost identical to that of Co(II)Cbl + WT *Lr*PduO devoid of ATP, in particular with regard to the region that is dominated by corrin $\pi \rightarrow \pi^*$ transitions. Since this region serves as a probe of the corrin ring conformation (see above), our data suggest that the R132K substitution causes ATP to become less rigidly bound. Consistent with this hypothesis, the $F1_{4c}$ feature exhibited by the 4c $Co(II)Cbi^+$ species in the R132K *Lr*PduO/ATP complex is red-shifted (by 67 cm^{-1}) from that observed for $Co(II)Cbi^+$ + WT *Lr*PduO/ATP, most likely signifying a more destabilized Co $3d_{x^2-y^2}$-based MO in the variant. While the X-ray crystal structures of the WT and R132K *Lr*PduO/ATP complexes do not actually show any noticeable differences with respect to the positioning of ATP,[33] it is expected that the binding of Co(II)Cbl or $Co(II)Cbi^+$ to the variant will cause a displacement of the more loosely bound cosubstrate. Also, it should be noted that the R132K *Lr*PduO/ATP crystal structure was obtained for a monomeric form of the enzyme. In the WT *Lr*PduO/ATP complex, ATP interacts with the R132 residue located in the adjacent subunit; hence, in the absence of protein oligomerization, the effect of the R132K substitution on the positioning of ATP cannot be evaluated on the basis of X-ray crystallographic data. It can, however, be inferred from our data, as the fact that 4c $Co(II)Cbi^+$ is formed in the R132K *Lr*PduO/ATP complex provides compelling evidence that this variant adopts the wild-type like oligomeric structure in solution.

The fraction of 4c $Co(II)Cbi^+$ that is formed in the R128K and D35N *Lr*PduO/ATP complexes remains high, even though both of these variants possess a perturbed salt bridge between adjacent subunits (Figure 1). In contrast, the relative population of 4c Co(II)Cbl in the *Lr*PduO/ATP complex is ∼10-fold reduced by the R128K substitution and completely suppressed by the D35N substitution (Table 1). The predominance of 5c Co(II)Cbl in these two variants is likely due to a failure of the active site to exclude the DMB moiety rather than a lack of Co(II)Cbl binding to the enzyme, since

dx.doi.org/10.1021/ic202096x | *Inorg. Chem.* 2012, 51, 4482−4494

the corresponding MCD spectra differ substantially from that of free Co(II)Cbl (Figures 4a and 5a).

4.1.3. Partial Damage of Hydrophobic Wall below Corrin Ring Plane. As expected on the basis of the X-ray crystal structure of substrate-bound *Lr*PduO,[31] the presence of F112 is critical with respect to the formation of 4c Co^{2+}corrinoids. However, the results obtained in the present study indicate that other amino-acid residues situated below the corrin ring plane also play an important role in this process. Specifically, the MCD spectra of Co(II)Cbl in the presence of the V186A and F187A *Lr*PduO/ATP complexes lack the $F1_{4c}$ feature characteristic of 4c Co^{2+}corrinoids; rather, they are quite similar to the free Co(II)Cbl MCD spectrum (Figures 6 and 10). This finding suggests that a partial damage to the hydrophobic wall drastically lowers the affinity of *Lr*PduO for Co(II)Cbl, presumably because the active sites of these variants can no longer promote the dissociation of the DMB ligand from the Co^{2+} ion, while at the same time they are somewhat too crowded to accommodate 5c, DMB-on Co(II)Cbl (note, however, that the F187A *Lr*PduO variant maintains significant catalytic activity at room temperature).[33] The V186A and F187A *Lr*PduO variants are, nonetheless, still capable of binding $Co(II)Cbi^+$ and of converting at least a fraction of this substrate analogue to the 4c state, as evidenced by the appearance of the $F1_{4c}$ feature in the corresponding MCD spectra. Yet, this feature is slightly shifted from its position in the $Co(II)Cbi^+$ + WT *Lr*PduO/ATP spectrum (Table 1), indicating that a partial damage to the hydrophobic wall also causes a small change in the positioning of the 4c $Co(II)Cbi^+$ species.

4.2. Mechanism of Formation of 4c Co^{2+}Corrinoids. Our results indicate that unlike Co(II)Cbl, the substrate analogue $Co(II)Cbi^+$ is still converted to a 4c species within the *Lr*PduO/ATP complex when the salt bridge or the hydrophobic wall of the active site are perturbed. The relative ease by which 4c $Co(II)Cbi^+$ is formed can be understood by considering the following two aspects. First and foremost, the axial ligand−Co^{2+} bond is stronger, and thus more difficult to break, in Co(II)Cbl than in $Co(II)Cbi^+$, because the DMB moiety is a much stronger base than a water molecule. Second, the distortion of the corrin ring needed to achieve the relatively planar conformation favored by the *Lr*PduO/ATP active site (ϕ = 5.7°, see above)[31] is presumably much larger for Co(II)Cbl (ϕ = 14.5°)[43] than for $Co(II)Cbi^+$ (no X-ray structural data available; however, note that ϕ = 6° for the only crystallographically characterized incomplete Co^{2+}corrinoid species, Co^{2+}cobyrinate[44]). Moreover, because of the steric bulk of the DMB ligand, a flattening of the corrin ring is energetically much more demanding for Co(II)Cbl than for $Co(II)Cbi^+$ and must therefore be coupled to axial ligand dissociation, which requires a higher level of coordination among the *Lr*PduO active-site residues to generate 4c Co(II)Cbl. As a result, even relatively subtle changes in the *Lr*PduO active site can induce a significant shift in the equilibrium between the enzyme-bound 5c and 4c Co(II)Cbl species.

Since most *Lr*PduO variants included in this study are still capable of generating a 4c $Co(II)Cbi^+$, we can construct an energy-level diagram that depicts the free energy of the 4c species relative to that of its 5c counterpart (Figure 13). In this approach, we assumed that the intensity of the $F1_{4c}$ feature is insignificantly affected by active-site amino acid substitutions, in which case the $\Delta\varepsilon$ value of this feature is proportional to the

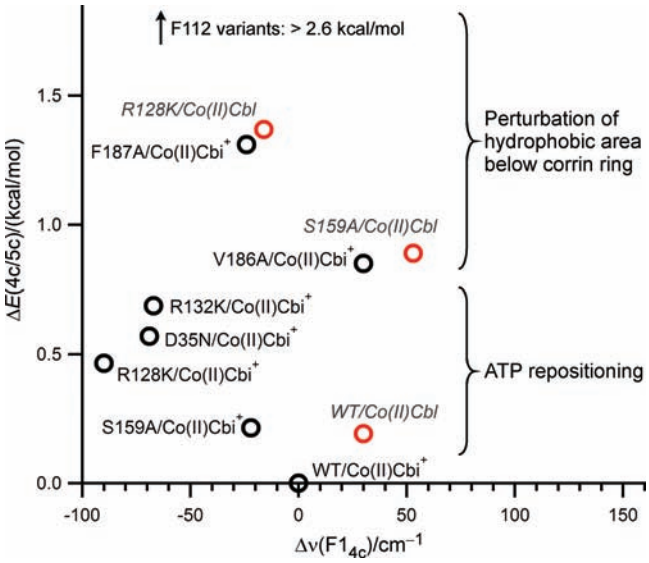

Figure 13. Plot of the difference in free energy, ΔE(4c/5c), between the 4 and 5c Co^{2+}corrinoids in each *Lr*PduO species investigated (all in the presence of cosubstrate ATP). Also shown is the shift of the $F1_{4c}$ feature, $\Delta\nu(F1_{4c})$, from its position in the Co^{2+}corrinoids + WT *Lr*PduO/ATP MCD spectra.

amount of 4c species present in a given sample. In our previous study of WT *Lr*PduO,[15] it was found that the yield of conversion from 5c to 4c Co^{2+}corrinoids in the presence of ATP is ∼40% for Co(II)Cbl and ∼50% for $Co(II)Cbi^+$ (Table 1). Therefore, by comparing the $\Delta\varepsilon$ values of the $F1_{4c}$ feature in the MCD spectra of the *Lr*PduO variants to those of Co(II)Cbl or $Co(II)Cbi^+$ in the WT *Lr*PduO/ATP complex ($\Delta\varepsilon$ = 193 and 225 M^{-1} cm^{-1}, respectively), the difference in free energy between the 4c and 5c Co^{2+}corrinoid species in each variant, ΔE(4c/5c), can be estimated (see Supporting Information, equations S1−S5). A plot of the ΔE(4c/5c) values obtained in this manner is shown in Figure 13. Since all spectra were obtained at the same temperature, these free energy differences provide direct insight into the effects of amino acid substitutions on enthalpic contributions to the equilibrium and thus on Co^{2+}corrinoid substrate/active site interactions. Above freezing point (250 K), the yield of conversion from 5c to 4c $Co(II)Cbi^+$ increases significantly in the WT *Lr*PduO/ATP complex due to entropic contributions, while in the case of Co(II)Cbl the temperature dependence of the equilibrium is negligible because the entropic changes associated with the dissociation of the intramolecular DMB ligand from the Co center are much smaller (Figure S5). Therefore, the fact that 4c Co(II)Cbl can be observed only in the R128K and S159A *Lr*PduO variants while most variants can form 4c $Co(II)Cbi^+$ shows that the effects of amino-acid substitutions on the reaction enthalpy (ΔH) associated with the 5c → 4c conversion are either much more dramatic for Co(II)Cbl than for $Co(II)Cbi^+$ or similar for both species but much more effectively compensated for by entropic contributions in the case of $Co(II)Cbi^+$. Although 4c Co(II)Cbl is only formed in a subset of *Lr*PduO variants, the fact that the trends in ΔE(4c/5c) values for Co(II)Cbl and $Co(II)Cbi^+$ follow the same order, namely, R128K > S159A > WT *Lr*PduO, suggests that active site amino-acid substitutions will similarly affect the relative stabilities of 4c Co(II)Cbl and 4c $Co(II)Cbi^+$. While at physiologically relevant temperatures changes in ΔH will

dx.doi.org/10.1021/ic202096x | *Inorg. Chem.* 2012, 51, 4482−4494

drastically affect the yield of 4c Co(II)Cbl formation, they can be partially compensated for by entropic contributions in the case of Co(II)Cbi$^+$.

Figure 13 underscores the significance of the F112 residue with respect to the enzyme-induced displacement of the axial ligand from the Co^{2+}corrinoids; both the F112A and the F112H *Lr*PduO variants are unable to produce any detectable amounts of a 4c species, even when Co(II)Cbi$^+$ is used as substrate. Additionally, as the area below the corrin ring becomes less hydrophobic, from the WT enzyme to the V186A, F187A, and, finally, the F112 *Lr*PduO variants, ΔE(4c/5c) increases sharply, causing a significant drop in the relative yield of formation of 4c Co(II)Cbi$^+$ and precluding the observation of any 4c Co(II)Cbl in these variants. Our data thus confirm that the residues involved in the hydrophobic wall below the corrin ring are crucial for the formation of 4c Co^{2+}corrinoids, as has been proposed previously on the basis of the X-ray crystal structure of Co(II)Cbl + WT *Lr*PduO/ATP.[31]

The decreased yield for the conversion from 5 to 4c Co^{2+}corrinoids in response to amino acid substitutions above or within the corrin ring plane (i.e., the R132K, S159A, R128K, and D35N substitutions) highlights the importance of the numerous hydrogen-bond interactions that exist between the corrin ring and the enzyme active site. Moreover, the relatively large ΔE(4c/5c) values for Co(II)Cbi$^+$ and, in particular, Co(II)Cbl bound to the R132K *Lr*PduO/ATP complex show that a proper positioning of the ATP molecule above the corrin ring is required to stabilize the 4c state. A perturbation, or complete rupture, of the salt bridge between adjacent subunits (D35N and R128K substitutions) causes relatively moderate changes in ΔE(4c/5c) for Co(II)Cbi$^+$, but drastically lowers the relative yield of formation of 4c Co(II)Cbl, especially in the case of the D35N substitution. This increased sensitivity of ΔE(4c/5c) for Co(II)Cbl over Co(II)Cbi$^+$ to a given amino acid substitution is preserved among all variants studied and consistent with our hypothesis that a higher level of coordination among the *Lr*PduO active-site residues is needed to generate 4c Co(II)Cbl (see above).

Substitutions of *Lr*PduO active-site residues not only modulate the intensity of the $F1_{4c}$ MCD feature, by lowering the yield of conversion from 5c to 4c Co^{2+}corrinoids, but also affect its position. As mentioned above, the $F1_{4c}$ feature of 4c Co^{2+}corrinoids was previously assigned as the Co $3d_{x^2-y^2} \rightarrow 3d_{z^2}$ LF transition; hence, a shift of this feature from its position in the Co^{2+}corrinoids + WT *Lr*PduO/ATP MCD spectra, $\Delta\nu(F1_{4c})$ can arise from a change in energy of the Co $3d_{x^2-y^2}$-based donor MO and/or the $3d_{z^2}$-based acceptor MO.[45] Given the lack of any axial bonding interactions in 4c Co^{2+}corrinoids, the energy of the latter MO should be relatively insensitive to active-site amino acid substitutions, and $\Delta\nu(F1_{4c})$ can therefore be used as a qualitative measure of corrin ring conformational changes in 4c Co^{2+}corrinoids. A plot of $\Delta\nu(F1_{4c})$ vs ΔE(4c/5c), which is included in Figure 13, shows that *Lr*PduO amino acid substitutions simultaneously affect both the ΔE(4c/5c) values and the corrin ring conformations of the enzyme-bound 4c Co^{2+}corrinoid species. As discussed in a recent paper,[46] it is quite common that enzyme activity and conformation are tightly coupled. However, in the present case no obvious relationship seems to exist between the $\Delta\nu(F1_{4c})$ and ΔE(4c/5c) values (which are representative of enzyme conformation and activity, respectively), which suggests that a moderate distortion of the corrin ring comes at a relatively low energetic cost and is unlikely to play a major role in the mechanism of formation of 4c Co^{2+}corrinoid species by the WT *Lr*PduO/ATP complex (note that CD spectroscopy is poorly suited to probe the suggested Co(II)corrinoid conformational changes due to the low symmetry of the corrin macrocycle).

By combing all of the above information, we can propose a molecular mechanism for the formation of 4c Co^{2+}corrinoids employed by *Lr*PduO. First, the binding of 4c Co^{2+}corrinoids to the WT *Lr*PduO/ATP complex has to be strongly favored thermodynamically, so as to compensate for the fact that the 5c, DMB- or water-bound Co^{2+}corrinoids are largely stabilized over their 4c counterparts in aqueous solution.[15,30] A clue as to how the binding of the Co^{2+}corrinoid substrate to the *Lr*PduO active site can provide the necessary driving force for displacing the axial ligand comes from a comparison to structurally characterized hemoproteins.[47] Usually, the binding of the heme cofactor to an apoenzyme is accompanied by the formation of a bond between the iron center of the heme and a basic amino-acid residue located in the active site. However, even the iron-free heme macrocycle, protoporphyrin IX, can bind to the active site of apo-myoglobin, because of the hydrophobic effect.[48] Specifically, the aromatic side chains in the active site of myoglobin, as well as other hemoproteins, can stabilize the bound porphyrin ring through π-stacking and/or edge-to-face interactions.[49] A similar hydrophobic effect is expected to be operative when Co(II)Cbl or Co(II)Cbi$^+$ bind to the *Lr*PduO/ATP complex. The crystal structures of WT *Lr*PduO complexed with ATP and Co^{2+}corrinoids show that several aromatic side chains, including those of F112, F187, Y163Y, and Y31, are located within close proximity to the corrin ring. Additionally, the crystal structure of the WT *Lr*PduO/ATP complex in the absence of Co^{2+}corrinoid substrates shows that the active site is occupied by water molecules, which will be released upon Co^{2+}corrinoid binding, thereby causing an overall increase in the entropy of the system.[14]

As the Co^{2+}corrinoid substrate enters the enzyme active site, the hydrophobic wall composed of F112, F187, and V186 in the C-terminal region and the ATP-bound pocket in the N-terminal region of the adjacent subunit reposition so as to cover both sides of the corrin ring, thereby promoting dissociation of the axial ligand. The nascent 4c Co^{2+}corrinoid species is stabilized further via equatorial hydrogen-bond interactions between the peripheral amide groups of the corrin ring and hydrophilic residues, such as R132 and S159, and the edge-to-face interactions between the corrin π system and aromatic residues, such as F112 and F187. According to this scenario, the salt bridge between D35 and R128 serves to hold all of these residues firmly in place, as otherwise the axial ligand, especially the DMB moiety, could enter the active site and remain coordinated to the Co^{2+} ion. The amino-acid substitution in hATR that is commonly found in patients who suffer from methylmalonic aciduria is structurally analogous to the R128W substitution in *Lr*PduO. On the basis of the results obtained in the present student for the R128K *Lr*PduO variant, this substitution likely disrupts the salt bridge between two subunits of hATR, thus allowing the axial DMB ligand of Co(II)Cbl to remain coordinated to the Co^{2+} ion. As a result, the reduction of Co(II)Cbl to Co(I)Cbl$^-$ is thermodynamically no longer feasible.

Finally, it should be noted that the level of control exerted by *Lr*PduO, and presumably ACAs in general, over the timing for the formation of the 4c Co^{2+}corrinoid intermediates is even more exquisite than we initially anticipated. While previous

dx.doi.org/10.1021/ic202096x | *Inorg. Chem.* 2012, 51, 4482–4494

spectroscopic studies conducted by us revealed that these "activated" Co^{2+}corrinoid intermediates are formed in high yield only in the presence of cosubstrate ATP,[15] we assumed that nucleotide analogues would still promote the formation of 4c Co^{2+}corrinoids in the enzyme active site and thus facilitate the $Co^{2+} \rightarrow Co^{1+}$ reduction step. However, the results obtained in this study provide compelling evidence that, at least in the case of *Lr*PduO, significant amounts of "activated" Co^{2+}corrinoid intermediates are formed only in the presence of ATP, which provides an additional safety mechanism for the enzyme active site to protect itself from being attacked by the transiently formed Co^{1+}corrinoid "supernucleophile".

■ ASSOCIATED CONTENT

Supporting Information

Additional EPR, Abs, and MCD spectra, chemical structure of the corrin ring, equations used to evaluate the difference in free energy, $\Delta E(4c/5c)$, between the 4- and 5c Co^{2+}corrinoids in each *Lr*PduO species, and validation of the approach used for estimating the relative populations of free and bound Co^{2+}corrinoids in a given sample and the relative populations of the 4c and 5c Co^{2+}corrinoid species of the enzyme-bound fraction. This material is available free of charge via the Internet at http://pubs.acs.org.

■ AUTHOR INFORMATION

Corresponding Author

*Phone: (608) 265-9056; fax: (608) 262-6143; e-mail: brunold@chem.wisc.edu.

Notes

The authors declare no competing financial interest.

■ ACKNOWLEDGMENTS

This work was supported in part by the National Science Foundation Grant MCB-0238530 (to T.C.B.) and the National Institutes of Health Grant R37-GM40313 (to J.C.E.-S.). P.E.M was supported in part by Grant F31-GM083668 from the National Institute of General Medical Sciences (NIGMS).

■ REFERENCES

(1) Banerjee, R. *Biochemistry* **2001**, *40*, 8634−8634.
(2) Chowdhury, S.; Banerjee, R. *Biochemistry* **2000**, *39*, 7998−8006.
(3) Marsh, E. N. G.; Ballou, D. P. *Biochemistry* **1998**, *37*, 11864−11872.
(4) Johnson, C. L. V.; Pechonick, E.; Park, S. D.; Havemann, G. D.; Leal, N. A.; Bobik, T. A. *J. Bacteriol.* **2001**, *183*, 1577−1584.
(5) Buan, N. R.; Suh, S. J.; Escalante-Semerena, J. C. *J. Bacteriol.* **2004**, *186*, 5708−5714.
(6) Thoma, N. H.; Evans, P. R.; Leadlay, P. F. *Biochemistry* **2000**, *39*, 9213−9221.
(7) Gerfen, G. J.; Licht, S.; Willems, J. P.; Hoffman, B. M.; Stubbe, J. *J. Am. Chem. Soc.* **1996**, *118*, 8192−8197.
(8) Brown, K. L.; Zou, X. *J. Inorg. Biochem.* **1999**, *77*, 185−195.
(9) Warren, M. J.; Raux, E.; Schubert, H. L.; Escalante-Semerena, J. C. *Nat. Prod. Rep.* **2002**, *19*, 390−412.
(10) Fenton, W. A.; Rosenberg, L. E. *Biochem. Biophys. Res. Commun.* **1981**, *98*, 283−289.
(11) Escalante-Semerena, J. C.; Suh, S. J.; Roth, J. R. *J. Bacteriol.* **1990**, *172*, 273−280.
(12) Dobson, C. M.; Wai, T.; Leclerc, D.; Kadir, H.; Narang, M.; Lerner-Ellis, J. P.; Hudson, T. J.; Rosenblatt, D. S.; Gravel, R. A. *Hum. Mol. Genet.* **2002**, *11*, 3361−3369.
(13) Suh, S. J.; Escalante-Semerena, J. C. *J. Bacteriol.* **1995**, *177*, 921−925.
(14) St Maurice, M.; Mera, P. E.; Taranto, M. P.; Sesma, F.; Escalante-Semerena, J. C.; Rayment, I. *J. Biol. Chem.* **2007**, *282*, 2596−2605.
(15) Park, K.; Mera, P. E.; Escalante-Semerena, J. C.; Brunold, T. C. *Biochemistry* **2008**, *47*, 9007−9015.
(16) Leal, N. A.; Park, S. D.; Kima, P. E.; Bobik, T. A. *J. Biol. Chem.* **2003**, *278*, 9227−9234.
(17) Walker, G. A.; Murphy, S.; Huenneke, F. *Arch. Biochem. Biophys.* **1969**, *134*, 95−102.
(18) Lawrence, A. D.; Deery, E.; McLean, K. J.; Munro, A. W.; Pickersgill, R. W.; Rigby, S. E. J.; Warren, M. J. *J. Biol. Chem.* **2008**, *283*, 10813−10821.
(19) Fonseca, M. V.; Escalante-Semerena, J. C. *J. Bacteriol.* **2000**, *182*, 4304−4309.
(20) Olteanu, H.; Wolthers, K. R.; Munro, A. W.; Scrutton, N. S.; Banerjee, R. *Biochemistry* **2004**, *43*, 1988−1997.
(21) Lexa, D.; Saveant, J. M. *Acc. Chem. Res.* **1983**, *16*, 235−243.
(22) McIver, L.; Leadbeater, C.; Campopiano, D. J.; Baxter, R. L.; Daff, S. N.; Chapman, S. K.; Munro, A. W. *Eur. J. Biochem.* **1998**, *257*, 577−585.
(23) Sampson, E. M.; Johnson, C. L. V.; Bobik, T. A. *Microbiology* **2005**, *151*, 1169−1177.
(24) Leal, N. A.; Olteanu, H.; Banerjee, R.; Bobik, T. A. *J. Biol. Chem.* **2004**, *279*, 47536−47542.
(25) Fonseca, M. V.; Escalante-Semerena, J. C. *J. Biol. Chem.* **2001**, *276*, 32101−32108.
(26) Mera, P. E.; Escalante-Semerena, J. C. *J. Biol. Chem.* **2010**, *285*, 2911−2917.
(27) Stich, T. A.; Buan, N. R.; Escalante-Semerena, J. C.; Brunold, T. C. *J. Am. Chem. Soc.* **2005**, *127*, 8710−8719.
(28) Stich, T. A.; Yamanishi, M.; Banerjee, R.; Brunold, T. C. *J. Am. Chem. Soc.* **2005**, *127*, 7660−7661.
(29) Stich, T. A.; Buan, N. R.; Brunold, T. C. *J. Am. Chem. Soc.* **2004**, *126*, 9735−9749.
(30) Liptak, M. D.; Brunold, T. C. *J. Am. Chem. Soc.* **2006**, *128*, 9144−9156.
(31) St Maurice, M.; Mera, P. E.; Park, K.; Brunold, T. C.; Escalante-Semerena, J. C.; Rayment, I. *Biochemistry* **2008**, *47*, 5755−5766.
(32) Schubert, H. L.; Hill, C. P. *Biochemistry* **2006**, *45*, 15188−15196.
(33) Mera, P. E.; Maurice, M. S.; Rayment, I.; Escalante-Semerena, J. C. *Biochemistry* **2007**, *46*, 13829−13836.
(34) Fan, C. G.; Bobik, T. A. *Biochemistry* **2008**, *47*, 2806−2813.
(35) Mera, P. E.; St Maurice, M.; Rayment, I.; Escalante-Semerena, J. C. *Biochemistry* **2009**, *48*, 3138−3145.
(36) Neese, F., University of Konstanz, 1997.
(37) Brooks, A. J.; Vlasie, M.; Banerjee, R.; Brunold, T. C. *J. Am. Chem. Soc.* **2005**, *127*, 16522−16528.
(38) Jensen, K. P.; Sauer, S. P. A; Liljefors, T.; Norrby, P. O. *Organometallics* **2001**, *20*, 550−556.
(39) Andruniow, T.; Zgierski, M. Z.; Kozlowski, P. M. *Chem. Phys. Lett.* **2000**, *331*, 509−512.
(40) Pett, V. B.; Liebman, M. N.; Murrayrust, P.; Prasad, K.; Glusker, J. P. *J. Am. Chem. Soc.* **1987**, *109*, 3207−3215.
(41) Brooks, A. J.; Vlasie, M.; Banerjee, R.; Brunold, T. C. *J. Am. Chem. Soc.* **2004**, *126*, 8167−8180.
(42) Stich, T. A.; Brooks, A. J.; Buan, N. R.; Brunold, T. C. *J. Am. Chem. Soc.* **2003**, *125*, 5897−5914.
(43) Krautler, B.; Keller, W.; Kratky, C. *J. Am. Chem. Soc.* **1989**, *111*, 8936−8938.
(44) Kräutler, B.; Keller, W.; Hughes, M.; Caderas, C.; Kratky, C. *J. Chem. Soc., Chem. Commun.* **1987**, 1678−1680.
(45) Note that because differences in the $F1_{4c}$ positions for the different variants investigated are generally very small, the extent of spin−orbit coupling among corresponding electronic states must remain largely unchanged, and thus, the intensity of the $F1_{4c}$ feature can be assumed to be constant.
(46) Benkovic, S. J.; Hammes, G. G.; Hammes-Schiffer, S. *Biochemistry* **2008**, *47*, 3317−3321.
(47) Reedy, C. J.; Gibney, B. R. *Chem. Rev.* **2004**, *104*, 617−649.

(48) Breslow, E.; Koehler, R.; Girotti, A. W. *J. Biol. Chem.* **1967**, *242*, 4149−4156.
(49) Liu, D. H.; Williamson, D. A.; Kennedy, M. L.; Williams, T. D.; Morton, M. M.; Benson, D. R. *J. Am. Chem. Soc.* **1999**, *121*, 11798−11812.